Efficient Content-Based Sparse Attention with Routing Transformers

Aurko Roy Mohammad Saffar Ashish Vaswani David Grangier

Google Research
{aurkor,msaffar,avaswani,grangier}@google.com

Abstract

Self-attention has recently been adopted for a wide range of sequence modeling problems. Despite its effectiveness, self-attention suffers from quadratic computation and memory requirements with respect to sequence length. Successful approaches to reduce this complexity focused on attending to local sliding windows or a small set of locations *independent* of content. Our work proposes to learn dynamic sparse attention patterns that avoid allocating computation and memory to attend to content unrelated to the query of interest. This work builds upon two lines of research: It combines the modeling flexibility of prior work on *content-based* sparse attention with the efficiency gains from approaches based on *local, temporal* sparse attention. Our model, the Routing Transformer, endows self-attention with a sparse routing module based on online k-means while reducing the overall complexity of attention to $O(n^{1.5}d)$ from $O(n^2d)$ for sequence length n and hidden dimension d. We show that our model outperforms comparable sparse attention models on language modeling on `Wikitext-103` (15.8 vs 18.3 perplexity), as well as on image generation on `ImageNet-64` (3.43 vs 3.44 bits/dim) while using fewer self-attention layers. Additionally, we set a new state-of-the-art on the newly released `PG-19` data-set, obtaining a test perplexity of 33.2 with a 22 layer Routing Transformer model trained on sequences of length 8192. We open-source the code for Routing Transformer in Tensorflow.[1]

1 Introduction

Generative models of sequences have witnessed rapid progress driven by the application of attention to neural networks. In particular, Bahdanau et al. (2015), Cho et al. (2014), and Vaswani et al. (2017) relied on attention to drastically improve the state-of-the art in machine translation. Subsequent research (Radford et al., 2018; Devlin et al., 2019; Liu et al., 2019; Yang et al., 2019) demonstrated the power of self-attention in learning powerful representations of language to address several natural language processing tasks. Self-attention also brought impressive progress for generative modeling outside of language, for example, image (Parmar et al., 2018; Menick and Kalchbrenner, 2018; Child et al., 2019) and music generation (Huang et al., 2018; Child et al., 2019).

Self-attention operates over sequences in a step-wise manner: At every time-step, attention assigns an *attention weight* to each previous input element (representation of past time-steps) and uses these weights to compute the representation of the current time-step as a weighted sum of the past input elements (Vaswani et al., 2017). Self-attention (Shaw et al., 2018) is a particular case of attention (Bahdanau et al., 2015; Chorowski et al., 2015; Luong et al., 2015).

Self-attention is commonly used in auto-regressive generative models. These models generate observations step-by-step, modeling the probability of the next symbol given the previously generated ones. At every time step, self-attentive generative models can directly focus on any part of the previous context. In contrast, recurrent neural networks (RNNs) and convolutional neural networks (CNNs) have direct interactions with only a local neighborhood of context around the current time step.

This advantage, however, comes at a price: Unlike recurrent networks or convolution networks, the time and space complexity of self-attention is quadratic in n, the length of the sequence. Specifically, for every position $i \leq n$, self-attention computes weights for its whole context of length i, which induces a complexity of $\sum_{i \leq n} i = n(n-1)/2$. This makes it difficult

[1] `https://github.com/google-research/google-research/tree/master/routing_transformer`.

Transactions of the Association for Computational Linguistics, vol. 9, pp. 53–68, 2021. https://doi.org/10.1162/tacl_a_00353
Action Editor: Xavier Carreras. Submission batch: 6/2020; Revision batch: 8/2020; Published 02/2021.

to scale attention-based models to modeling long sequences. However, long sequences are the norm in many domains, including music, image, speech, video generation, and document-level machine translation.

Therefore, an important research direction is to investigate sparse and memory efficient forms of attention in order to scale to tasks with large sequence lengths. Previous work has proposed *data independent* or fixed sparsity patterns bounding temporal dependencies, such as local or strided attention. At each time step, the model attends only to a fixed number of time steps in the past (Child et al., 2019). Extensions to local attention have suggested learning the length of the temporal sparsity for each attention module in the network (Sukhbaatar et al., 2019). These strategies draw their inspiration from RNNs and CNNs and bound their complexity by attending only to representations summarizing a *local* neighborhood of the current time step. Their attention matrices (matrices containing the attention weights for every pair of previous, current time-step) are natively sparse and require instantiating only non-zero entries. While these approaches have achieved good results, fixing the sparsity pattern of a content based mechanism such as self-attention can limit its ability to pool in information from large contexts.

As an alternative to local attention, Correia et al. (2019) consider content-based sparsity, an approach allowing for arbitrary sparsity patterns. This formulation, however, does require instantiating a full dense attention matrix prior to sparsification through variants of L_0-sparsity or sparsemax approximations (Blondel et al., 2019).

The present work builds upon these two lines of research and proposes to retain the modeling flexibility of content-based sparse attention while leveraging the efficiency of natively sparse attention matrices. Our formulation avoids sparsemax variants and relies on clustering of attention instead. Each attention module considers a clustering of the space: The current time-step only attends to context belonging to the same cluster. In other words, the current time-step query is *routed* to a limited number of context elements through its cluster assignment. This strategy draws inspiration from the application of spherical k-means clustering to the Maximum Inner Product Search (MIPS) problem.

Our proposed model, Routing Transformer, combines our efficient clustering-based sparse attention with classical local attention to reach excellent performance both for language and image generation. These results are obtained without the need to maintain attention matrices larger than batch length which is the case with the segment level recurrence mechanism used in Dai et al. (2019) and Sukhbaatar et al. (2019). We present experimental results on language modeling (`enwik-8`, `Wikitext-103`, and `PG-19`) and unconditional image generation (`CIFAR-10` and `ImageNet-64`). Routing Transformer sets new state-of-the-art, while having comparable or fewer number of self-attention layers and heads, on `Wikitext-103` (15.8 vs 18.3 perplexity), `PG-19` (33.2 vs 33.6 perplexity), and on `ImageNet-64` (3.43 vs 3.44 bits/dim). We also report competitive results on `enwik-8` (0.99 vs 0.98 perplexity) and present ablations on `CIFAR-10`.

2 Related Work

Attention with Temporal Sparsity: Research on efficient attention neural models parallels the advent of attention-based architectures. In the context of speech recognition, Jaitly et al. (2016) proposed the Neural Transducer, which segments sequences in non-overlapping chunks and attention is performed in each chunk independently. Limiting attention to a fixed temporal context around the current prediction has also been explored in Chorowski et al. (2015), while Chiu and Raffel (2018) dynamically segment the sequence into variable sized-chunks.

Hierarchical attention strategies have also been explored: The model first considers which part of the inputs should be attended to before computing full attention in a contiguous neighborhood of the selected area (Gregor et al., 2015; Xu et al., 2015; Luong et al., 2015). Later, hierarchical attention, simplified by Liu et al. (2018), alternates coarse layers (attending to the whole sequence at a lower temporal resolution) with local layers (attending to a neighborhood of the current prediction).

This alternating strategy is also employed by Child et al. (2019), who introduce bounded and strided attention, namely, attending to a fixed context in the past at a sub-sampled temporal resolution. This work formalizes such a strategy

using a sparse attention formalism, showing how it relates to full attention with a specific sparsity pattern in the attention matrix. It shows that sparse attention is sufficient to get state-of-the-art results in modeling long sequences over language modeling, image generation and music generation. Sukhbaatar et al. (2019) build upon this work and show that it is possible to obtain further sparsity by letting the model learn the length of the temporal context for each attention module. This work also makes use of the attention cache introduced in Dai et al. (2019), a memory mechanism to train models over temporal contexts which extend beyond the length of the training batches.

Attention with Content-Based Sparsity: The above work mainly relies on two efficient ideas: attending to less elements by only considering a fixed bounded local context in the past, and attending to less elements by decreasing the temporal resolution of context. These ideas do not allow arbitrary sparsity patterns in attention matrices. Content-based sparse attention has been introduced to allow for richer patterns and more expressive models. (Martins and Kreutzer (2017) and Malaviya et al. (2018)) propose to compute attention weights with variants of sparsemax. Correia et al. (2019) generalize this approach to every layer in a Transformer using entmax which allows for more efficient inference. This line of work allows for learning arbitrary sparsity attention patterns from data, based on the content of the current query and past context. However, sparsity here cannot be leveraged to improve space and time complexity because sparsemax/entmax formulations require instantiating the full attention matrix prior to sparsification. This is a drawback compared with temporal sparsity approaches. Our work is motivated by bridging this gap and allows for arbitrary sparsity patterns while avoiding having to instantiate non-zero entries of attention matrices.

Contemporaneous to our work, Kitaev et al. (2020) proposed to use Locality Sensitive Hashing (LSH) using random hyperplanes to infer content based sparsity patterns for attention: tokens that fall into the same hash bucket, get to attend to each other. While similar in spirit to our approach, the approach of Kitaev et al. (2020) keeps the randomly initialized hyperplanes fixed throughout, while we use mini-batch spherical k-means to learn the space-partitioning centroids. The motivation in both approaches is to approximate MIPS in the context of dot product attention, for which both LSH and spherical k-means have been used in literature. However, typically spherical k-means is known to outperform LSH for MIPS (see, e.g., Auvolat et al., 2015). This is borne out in the common task of `Imagenet-64` generation, where Reformer gets around 3.65 bits/dim (Figure 3), while the Routing Transformer gets 3.43 bits/dim (see Table 4 for a comparison).

Sparse Computation beyond Attention: Learning models with sparse representations/ activations for saving time and computation has been addressed in the past in various contexts. Previous work often refers to this goal as *gating* for conditional computation. Gating techniques relying on sampling and straight-through gradient estimators are common (Bengio et al., 2013; Eigen et al., 2013; Cho and Bengio, 2014). Conditional computation can also be addressed with reinforcement learning (Denoyer and Gallinari, 2014; Indurthi et al., 2019). Memory augmented neural networks with sparse reads and writes have also been proposed in Rae et al. (2016) as a way to scale Neural Turing Machines (Graves et al., 2014). In the domain of language modeling, a related work is the sparsely gated Mixture-of-experts (MOE) (Shazeer et al., 2017), where sparsity is induced by *experts* and a trainable gating network controls the routing strategy to each sub-network. Another related work is Lample et al. (2019) who use product quantization based key-value lookups to replace the feed forward network in the Transformer. Our work differs from theirs in that we make use of dynamic key-value pairs to infer sparsity patterns, while their key-value pairs are the same across examples.

3 Self-Attentive Auto-regressive Sequence Modeling

Auto-regressive sequence models decompose the probability of a sequence $\mathbf{x} = (x_1, \ldots, x_n)$ as

$$p(\mathbf{x}) = p_\theta(x_1) \prod_{i=2}^{n} p_\theta(x_i | x_{<i}). \qquad (1)$$

In neural models, the conditional distribution $p_\theta(x_i|x_{<i})$ is modeled by a neural network with learned parameters θ and these parameters are typically learned to maximize the likelihood of the training data. In particular, Transformer

architectures have shown to reach state-of-the-art accuracy in several domains, including language modeling (Vaswani et al., 2017; Radford et al., 2018), image generation (Parmar et al., 2018), and music generation (Huang et al., 2018). Transformer models compose a series of attention modules. Each module refines the input representation by taking a weighted average of the representations from the previous modules.

For every module, the input representation is a sequence of n vectors $\mathbf{x} = (x_1, \ldots, x_n)$ from a continuous space of dimension d. Thus one may actually treat the input sequence as a $n \times d$ matrix X. A self-attention layer operates on this representation. It first applies three linear projections,

$$Q = XW_Q, \quad K = XW_K, \quad V = XW_V, \quad (2)$$

where Q, K, and V are referred to as *keys*, *queries*, and *values*, while W_Q, W_K, and W_V are learned projection matrices.

The key and the query matrices determine the $n \times n$ attention matrix $A = \mathrm{softmax}\left(QK^\top\right)$, where the softmax operator over matrices denotes that the softmax function has been applied to each row. In the case of self-attention for auto-regressive models, queries attend only over keys from previous time-steps, that is,

$$A = \mathrm{softmax}\left(\mathrm{ltr}(QK^\top)\right), \quad (3)$$

where ltr denotes the lower triangular operator. The attention matrix A may be interpreted as a matrix of weights in $[0, 1]$ where A_{ij} denotes how much query position i at the next layer must pay attention to key position j at the previous layer. Given the attention matrix A, the next layer representation X' is then computed simply as AV. In summary,

$$X'_i = \sum_{j<i}^{n} A_{ij} V_j. \quad (4)$$

In practice, Transformer (Vaswani et al., 2017) adds several extensions to this basic self-attention mechanism. In particular, the result X' of performing self-attention is scaled by $1/\sqrt{d}$. Moreover, each layer relies on multiple attention *heads*, that is, each layer performs multiple projections onto triplet (queries, keys, values) and attention is performed for each head. The attention results from all heads are then concatenated. This strategy allows each head to specialize on different aspects of the input sequence. In addition, Transformer further processes the result of attention through a learnable nonlinear transformation (multilayer perceptron, mlp) followed by a residual connection and a normalization step, namely,

$$X' = \mathrm{layernorm}(X' + X) \quad (5)$$

$$X'' = \mathrm{layernorm}(\mathrm{mlp}(X') + X), \quad (6)$$

where $\mathrm{layernorm}$ denotes the parameterized normalization step from Ba et al. (2016). A full Transformer model is therefore a chain of attention modules (Eq. 6) preceded by an embedding module (learnable representation for symbols and their positions) and followed by a logistic classification module (learnable linear classifier to predict the next symbol).

Our work is interested in the application of the Transformer to long sequences, a challenging problem since space and time complexity of attention is quadratic in sequence length n. We describe various approaches to sparse attention including ours in the next section.

4 Efficient Content-Dependent Sparse Attention

Attention-based models can be problematic for long sequences. For a sequence of length n, the full attention matrix A, as introduced in Section 3, is $n \times n$-dimensional and can be prohibitive to instantiate. This motivates sparse attention models, that is, models relying on attention matrices which have a majority of zero entries.

For each query, a sparse attention model defines a set of keys that can be attended to. In the following, we introduce the set S_i as the set of key positions that the query at position i can attend to, namely,

$$X'_i = \sum_{j \in S_i} A_{ij} V_j. \quad (7)$$

The set of all such key positions defines a sparsity pattern $\mathcal{S} = \{S_i \mid 1 \leq i \leq n\}$ for the entire sequence. For example, classical causal self attention can attend to every key prior to the current query, which translates to

$S_i = \{j \mid j < i\}$ for every i. Most previous work on attention sparsity defined such sets purely based on positions, independently of actual query and key vectors. For example, local attention (Luong et al., 2015) considers attending only to a k-long time window prior to the current query, $S_i = \{j \mid i - k \leq j < i\}$ for every i. The work of Child et al. (2019) proposes block sparse attention where half the heads perform local attention, and half the heads perform *strided attention* given by $S_i = \{j \mid i - j \pmod k = 0, j < i\}$ for every i. The approach of Sukhbaatar et al. (2019) is also a variant of local attention where the cardinality of $|S_i|$ is learned from data with an L_1 penalty to trade-off sparsity with modeling accuracy.

These *local* attention sparsity variants are effective in practice since correlation between observations naturally decrease with time for many problems. In our experiments, we actually find that local attention is a surprisingly strong baseline in both image generation and language modeling: for example, a scaled up ImageTransformer (Parmar et al., 2018) gets 3.48 bits/dim compared to the 3.44 bits/dim reported in Child et al. (2019). Similarly, scaled up versions of Transformer with local attention and the relative positional encoding scheme of Shaw et al. (2018) are able to get 19.8 perplexity on `Wikitext-103`, 1.10 bits per byte on `enwik-8`, and 39.3 on `PG-19`, while Transformer-XL (Dai et al., 2019) gets 18.3, 0.99, and 36.3 respectively. From an efficiency perspective, local attention is also interesting because sparsity patterns are regular, contiguous in memory, and known in advance.

In this work, however, we are interested in a more generic formulation of attention sparsity and would like the sparsity pattern to be informed by the data, namely, $\mathcal{S} = f(\mathbf{x})$. This approach has several modeling advantages: It can accommodate data without a clear ordering over observations. For temporal data, it can also discover patterns with greater sparsity if some types of queries have a longer lasting effect on future observations than others. Content-based sparse attention should, however, be carefully implemented if we need to avoid instantiating full attention matrices at any point in time. For instance, Correia et al. (2019) infer sparsity from data but their formulation instantiates a full attention matrix before finding its sparse counterpart. The next section explains how a natively sparse approach can actually be devised inspired by the MIPS problem.

4.1 Routing Attention with Clustering

Our strategy follows the motivation we delineated in the previous section: We model sparse attention matrices with a low rank sparsity patterns relying on k-means clustering. Our strategy first assigns queries and keys to clusters. Then only queries and keys from the same cluster are considered for attention.

Precisely, our model clusters both keys K and queries Q using mini-batch k-means clustering on the same set of centroid vectors $\boldsymbol{\mu} = (\mu_1, \cdots, \mu_k) \in \mathbb{R}^{k \times d}$. These centroid parameters are model parameters and are shared across sequences. They are learned online along with the rest of the parameters, as delineated in Bottou and Bengio (1995). Once cluster membership for queries and keys are determined, we denote by $\mu(Q_i) \in \boldsymbol{\mu}$ the nearest centroid to Q_i and by $\mu(K_j) \in \boldsymbol{\mu}$ the nearest centroid to K_j. This allows us to define our sparse attention strategy as

$$X_i' = \sum_{\substack{j : K_j \in \mu(Q_i), \\ j < i}} A_{ij} V_j. \tag{8}$$

In summary, queries are routed to keys belonging to the same cluster. To see the connection with MIPS, we recall the setting of the MIPS problem adapted to the case of dot-product attention. In this problem we are given a large collection of vectors $\mathcal{K} = \{K_1, \cdots, K_n\}$ of size n in $\mathbb{R}^d$ and for a given query $Q_i \in \mathbb{R}^d$, we are interested in searching for a key $K_j \in \mathcal{K}$ which (approximately) maximizes $Q_i^\top K_j$:

$$K_j = \arg\max_{x \in \mathcal{K}} Q_i^\top x. \tag{9}$$

The MIPS problem is useful in the dot product attention setting because the importance of a particular key K_j to a query Q_i is directly proportional to its dot product $Q_i^\top K_j$. Thus given a budget of items that a query Q_i can attend to, the optimal choice of keys K_j are the ones given by the MIPS objective in Equation 9. The motivation for using k-means clustering, is the observation that the MIPS problem is equivalent to the Nearest Neighbor Search problem when the norm of every element $K_j \in \mathcal{K}$ is constant.

Therefore, we work with queries and keys which are unit vectors, projecting them onto the unit ball, immediately before computing them. In practice, instead of normalizing by the ℓ_2 norm, we use Layer Normalization (Ba et al., 2016) with the

scale and bias terms disabled. This has the benefit of projecting vectors in $\mathbb{R}^d$ to the d-ball and prevents its entries from becoming too small. These layer normalized keys and queries are also used subsequently for computing the dot product attention. Note that performing k-means algorithm on unit vectors is equivalent to the *spherical* k-means algorithm. Projecting queries and keys to the unit ball implies that:

$$\|Q_i - K_j\|^2 \tag{10}$$

$$= \|Q_i\|^2 + \|K_j\|^2 - 2Q_i^\top K_j \tag{11}$$

$$= 2 - 2\left(Q_i^\top K_j\right). \tag{12}$$

Thus if Q_i and K_j belong to the same cluster center (i.e., $\mu(Q_i) = \mu(K_j) = \mu$), then it follows that there is some $\varepsilon > 0$, such that $\|Q_i - \mu\|, \|K_j - \mu\| < \varepsilon$. This implies via triangle inequality that:

$$\|Q_i - K_j\| \leq \|Q_i - \mu\| + \|K_j - \mu\| < 2\varepsilon. \tag{13}$$

Thus, from Equation 12 it follows that, $Q_i^\top K_j > 1 - 2\varepsilon^2$. Therefore, when two time steps $i > j$ are assigned the same cluster due to a small $\|Q_i - \mu\|, \|K_j - \mu\|$ distance, it also means that their attention weight $Q_i^\top K_j$ is high, namely, K_j is an approximate solution to the MIPS objective of Equation 9 for query Q_i. This analysis shows that our clustering routing strategy preserves large attention weights as non-zero entries.

Because we route attention via spherical k-means clustering, we dub our model *Routing Transformer*. We give a detailed pseudo-code implementation for the routing attention computation in Algorithm 1. A visualization of the attention scheme and its comparison to local and strided attention is given in Figure 1. The computational complexity of this variant of sparse attention is $O(nkd + n^2 d/k)$. Cluster assignments correspond to the first term, that is, it compares n routing vectors to all k centroids in a space of size d. Query/key dot products corresponds to the second term, that is, assuming balanced clusters, each of the n queries is compared to n/k in its cluster through a dot product of dimension d. Therefore the optimal choice of k is $\sqrt{n}$ as in Child et al. (2019), thereby reducing overall memory and computational cost to $O\left(n^{1.5}d\right)$ instead of $O(n^2 d)$ (Vaswani et al., 2017).

In practice, we apply mini-batch k-means to train the cluster centroids. However, in order to infer balanced routing patterns, we define the sets S_i to be of equal size roughly $n/k \sim \sqrt{n}$, that is, for every centroid μ_i we sort tokens by distance to μ_i and cluster membership is determined by this threshold (top-k). This adds an additional $O(n \log n)$ term to the cost, however note that this is eclipsed by the dominating term of $O(n^{1.5}d)$. This strategy is simple and efficient. In particular, it guarantees that all clusters have the same size, which is extremely important in terms of computational efficiency on parallel hardware like graphic cards. As a downside, this assignment does not guarantee that each point belongs to a single cluster. In the future, we want to investigate using balanced variants of k-means (Banerjee and

Algorithm 1 Routing Attention

Queries, Keys and Values: $Q, K, V \in \mathbb{R}^{n \times d}$
Centroid: $\boldsymbol{\mu} \in \mathbb{R}^{k \times d}$
decay: λ
if `left to right mask` **then**
    $K \leftarrow Q$
▷ Normalize to unit ball
$Q \leftarrow \mathrm{LayerNorm}(Q)$ ▷ scale, bias disabled
$K \leftarrow \mathrm{LayerNorm}(K)$ ▷ scale, bias disabled
$Q_{prod} \leftarrow \boldsymbol{\mu} Q^\top$ ▷ $k \times n$
if `not left to right mask` **then**
    $K_{prod} \leftarrow \boldsymbol{\mu} K^\top$ ▷ $k \times n$
$w \leftarrow n/k$ ▷ attention window
$Q_{idx} \leftarrow \text{top-k}(Q_{prod}, w)$ ▷ $k \times w$
$Q_{idx} \leftarrow \mathrm{sort}(Q_{idx})$ ▷ sort to preserve order
$K_{idx} \leftarrow Q_{idx}$ ▷ $k \times w$
if `not left to right mask` **then**
    $K_{idx} \leftarrow \text{top-k}(K_{prod}, w)$ ▷ $k \times w$
    $K_{idx} \leftarrow \mathrm{sort}(K_{idx})$ ▷ sort to preserve order
$Q' \leftarrow \mathrm{gather}(Q, Q_{idx})$ ▷ $k \times w \times d$
$K' \leftarrow \mathrm{gather}(K, K_{idx})$ ▷ $k \times w \times d$
$V' \leftarrow \mathrm{gather}(V, K_{idx})$ ▷ $k \times w \times d$
$A \leftarrow Q'(K')^\top$ ▷ $k \times w \times w$
if `left to right mask` **then**
    $A \leftarrow \mathrm{ltr}(A)$
$A \leftarrow \mathrm{softmax}(A)$. ▷ $k \times w \times w$
$V' \leftarrow \mathrm{einsum}(kww, kwd \rightarrow kwd, A, V')$
$X \leftarrow \mathrm{scatter}(K_{idx}, V')$
$Q_m \leftarrow \text{one-hot}(\arg\max(Q_{prod}))$ ▷ $k \times n$
$K_m \leftarrow \text{one-hot}(\arg\max(K_{prod}))$ ▷ $k \times n$
▷ Update centroids
$\boldsymbol{\mu} \leftarrow \lambda\boldsymbol{\mu} + (1-\lambda)Q_m Q/2 + (1-\lambda)K_m K/2$
return X

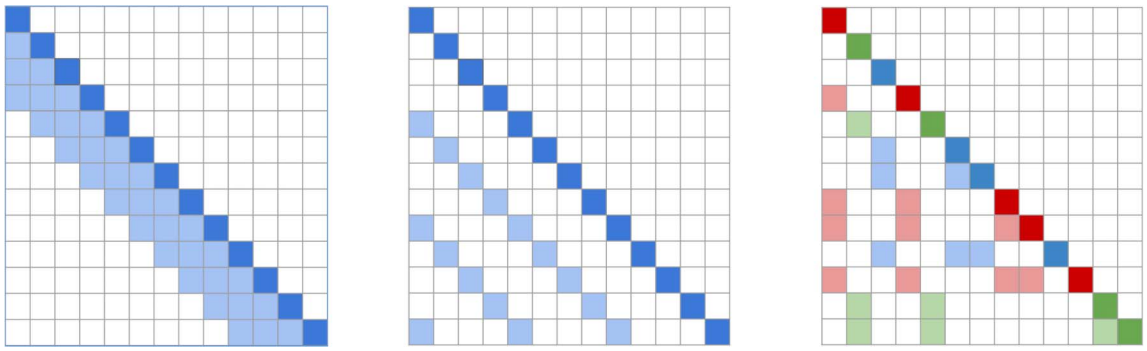

(a) Local attention (b) Strided attention (c) Routing attention

Figure 1: Figures showing 2-D attention schemes for the Routing Transformer compared to local attention and strided attention of (Child et al., 2019). The rows represent the outputs while the columns represent the inputs. For local and strided attention, the colored squares represent the elements every output row attends to. For attention routed as in Section 4.1, the different colors represent cluster memberships for the output token.

Ghosh, 2004; Malinen and Fränti, 2014) which is not common in an online setting.

During training, we update each cluster centroid μ by an exponentially moving average of all the keys and queries assigned to it:

$$\mu \leftarrow \lambda\mu + \frac{(1-\lambda)}{2}\sum_{i:\mu(Q_i)=\mu} Q_i + \frac{(1-\lambda)}{2}\sum_{j:\mu(K_j)=\mu} K_j,$$

where λ is a decay parameter that we usually set to 0.999. Additionally, we also exclude padding tokens from affecting the centroids.

There is an additional nuance regarding clustering queries and keys that comes into play when using causal attention (i.e., left to right masking), as is usually the case in language models. When grouping queries and keys belonging to a certain cluster centroid μ, we may get as members queries Q_i for keys K_j where time-step $i \leq j$. This therefore requires an additional masking strategy in addition to the lower triangular mask used for causal attention. One solution that avoids having to use an additional mask, is to simply share keys and queries. Empirically, we have found that this works at par or better than separate keys and queries together with an additional masking strategy in the causal attention setting. For encoder self attention and encoder-decoder cross-attention, additional masking or sharing queries and keys is not necessary.

5 Experiments

We evaluate our sparse attention model on various generative modeling tasks including text and image generation. The following sections report our results on `CIFAR-10`, `Wikitext-103` (Merity et al., 2017), `enwik-8` (Mahoney, 2011), `ImageNet-64`, as well as `PG-19` (Rae et al., 2020). We find that a scaled up version of local attention is a surprisingly strong baseline and that our Routing Transformer outperforms Transformer-XL (Dai et al., 2019) and the Sparse Transformer model of Child et al. (2019) on all tasks. On the recently released `PG-19` data-set, we find that local attention again is a strong baseline, with a slightly worse performance compared to Transformer-XL (Dai et al., 2019). We also find that the Routing Transformer model outperforms both Transformer-XL (Dai et al., 2019) and Compressive Transformer (Rae et al., 2020), setting a new state-of-the-art result.

In all our models except the one used for `PG-19`, we allocate half the heads to do local attention and the other half to route attention as in Equation 8. For all our experiments except for `PG-19`, we use the Adam optimizer (Kingma and Ba, 2015) with learning rate 2×10^{-4} with $\beta_1 = 0.9$ and $\beta_2 = 0.98$ following the learning rate schedule described in Vaswani et al. (2017). We train all models on 128 TPUv3 cores. The setup used for `PG-19` is described in Section 5.5.

5.1 CIFAR-10

`CIFAR-10` is a widely used image data-set that consists of 60,000 colored images of size 32×32. Since the sequence lengths in this case are relatively short (3072), we use this as a toy data-set to perform various ablations to tease apart the effect of various hyperparameter choices

Model	Routing heads	Routing Layers	Attention window	Bits/dim	Steps/sec
Transformer	0	0	3072	2.983	5.608
Local Transformer	0	0	512	3.009	9.023
Random Transformer	4 (random)	8 (random)	512	3.076	5.448
Routing Transformer	2	2	512	3.005	7.968
Routing Transformer	4	2	512	2.986	7.409
Routing Transformer	8	2	512	2.992	6.682
Routing Transformer	2	4	512	2.995	7.379
Routing Transformer	4	4	512	2.975	6.492
Routing Transformer	8	4	512	2.991	5.385
Routing Transformer	2	8	512	2.995	6.442
Routing Transformer	4	8	512	2.971	5.140
Routing Transformer	8	8	512	3.190	3.897
Routing Transformer	2	12	512	2.978	5.685
Routing Transformer	4	12	512	2.994	4.349
Routing Transformer	8	12	512	3.400	3.062
Routing Transformer	2	2	1024	2.975	7.344
Routing Transformer	4	2	1024	2.950	6.440
Routing Transformer	8	2	1024	2.982	5.192
Routing Transformer	2	4	1024	2.990	6.389
Routing Transformer	4	4	1024	2.958	5.112
Routing Transformer	8	4	1024	3.003	3.674
Routing Transformer	2	8	1024	2.991	5.057
Routing Transformer	4	8	1024	2.983	3.597
Routing Transformer	8	8	1024	3.131	2.329
Routing Transformer	2	12	1024	2.973	4.151
Routing Transformer	4	12	1024	3.005	2.788
Routing Transformer	8	12	1024	3.291	1.711

Table 1: Ablation studies of the Routing Transformer model on the `CIFAR-10` data-set. All the models have a total of 12 attention layers and 8 heads. Routing layers when present are always added at the top of the model. A Routing Transformer model with less than 12 routing attention layers and less than 8 routing heads, has the remaining layers and heads of type local attention. A Random Transformer model has a random attention head in place of the routing attention head. We report the performance in bits/dim on the test set and step times are reported on a TPUv3.

on the model performance. We train 12 layer models with a total of 8 attention heads, and report a comparison of the effect of various hyper-parameter choices on the performance and speed on this data-set. In particular, the following hyper-parameters are varied 1) the number of routing attention heads, 2) the number of routing attention layers, and 3) the size of the attention window. For routing attention we use $k = 6$ while varying the attention window, to see the effect on speed and performance. All the `CIFAR-10` models are trained with a batch size of 32 and for a total of 200,000 steps. In addition, we also compare the Routing Transformer to a *Random Transformer*, where K_{idx} is randomly chosen rather than being drawn from nearest neighbor search. For a fair comparison, we take the best model from Table 1, with an attention window of 512 and replace all routing heads with *random heads*. We present the ablation results in Table 1 and discuss it in more detail in Section 6.

5.2 Wikitext-103

`Wikitext-103` (Merity et al., 2017) is a large public benchmark data-set for testing long term dependencies in word-level language models. It contains over 100 million tokens from 28K articles extracted from Wikipedia with an average of 3.6K tokens per article, which makes it a reference data-set to model long-term textual dependencies. We

train a 10 layer Routing Transformer with 16 heads using the relative position encoding of Shaw et al. (2018) and with attention and ReLU dropout rate of 0.3 each. For routing attention as in Section 4.1 we choose $k = 16$ and attention window to be 256 during both training and evaluation. We describe our results in Table 2 and compare it to other recent work on sparse or recurrent attention such as Adaptive Inputs (Baevski and Auli, 2019) and TransformerXL (Dai et al., 2019) as well as a local attention with relative position encoding baseline (Huang et al., 2018). We find that local attention is a great inductive bias for sparse attention and is better than the adaptive methods proposed in Baevski and Auli (2019); Sukhbaatar et al. (2019). Moreover, our Routing Transformer model is able to get a test perplexity of 15.8 improving on the 18.3 obtained by TransformerXL (Dai et al., 2019) while having fewer self-attention layers, and without the need for segment level recurrence.

5.3 enwik-8

The `enwik-8` (Mahoney, 2011) is a data-set to benchmark text compression algorithms in the context of the Hutter prize. This data-set consists of the first 100M bytes of unprocessed Wikipedia. It is typically used to evaluate character-level language models. Similar to the prior work of Dai et al. (2019) and Child et al. (2019) we use a sequence length $n = 8192$ and benchmark our results against various baselines including local attention. We train a 24 layer model with 8 attention heads with an attention and ReLU dropout rate of 0.4 each and using the relative position encoding of Shaw et al. (2018). For routing attention as in Section 4.1 we set $k = 32$ and attention window 256. We report perplexity of 0.99 like TransformerXL and Sparse Transformer, slightly under 0.98 from Adaptive Transformer.

5.4 ImageNet 64×64

In order to evaluate the ability of our model to capture long term dependencies on a modality other than text, we report results on the `ImageNet` 64×64 data-set as used in Child et al. (2019). For auto-regressive image generation, this data-set consists of images of $64 \times 64 \times 3$ bytes represented as long sequences of length 12,288 presented in raster scan, red-green-blue order. We train a 24 layer model with 16 attention heads, with half the heads performing local attention, and the other half routing attention as in Section 3. For routing attention we set $k = 8$, attention window 2048, batch size 1, and train our model for roughly 70 epochs as in Child et al. (2019). We compare our model to a scaled-up ImageTransformer model with local attention (Parmar et al., 2018) and the SparseTransformer model of Child et al. (2019).

We find that local attention (Parmar et al., 2018) is a strong baseline for image generation, obtaining 3.48 bits/dim when scaled up to 24 layers and 16 heads, compared to later work like Sub-scale Pixel Networks (SPN) (Menick and Kalchbrenner, 2018). Our Routing Transformer model achieves a performance of 3.425 bits/dim (see Table 4) compared to the previous state-of-the-art of 3.437 bits/dim (Child et al., 2019), thereby showing the advantage of the content based sparsity formulation of Section 4.1.

5.5 PG-19

`PG-19` is a new data-set released by Rae et al. (2020) which is larger and longer than previous language modeling data-sets. The data-set is created from approximately 28,000 Project Gutenberg books published before 1919, consisting of 1.9 billion tokens and comprises an average context size of roughly 69,000 words. This is text that is $10\times$ longer in context than all prior data-sets such as `Wikitext-103`, with minimal pre-processing and an open vocabulary that makes it extremely challenging for long text modeling tasks. We use a subword vocabulary of size approximately 98,000 and report perplexities normalized by the token counts reported in Rae et al. (2020). On this data-set we train a 22 layer Routing Transformer model with 8 heads with a sequence length of 8192 and set a new state-of-the-art result on this data-set, improving on both Compressive Transformers (Rae et al., 2020), as well as Transformer-XL (Dai et al., 2019). For this data-set we change our training setup in three ways. Firstly, we use only 2 routing heads instead of sharing it equally with local heads. Secondly, we use routing heads only in the last two layers of the model instead of having them present in every layer. This is motivated by our empirical finding that long range attention is only needed in the last few layers - see also Rae and Razavi (2020). Finally, we use the Adafactor optimizer (Shazeer and Stern, 2018) which is more memory efficient than Adam in training larger models. We use a learning rate constant of 0.01 with a

Model	Layers	Heads	Perplexity
LSTMs (Grave et al., 2017)	–	–	40.8
QRNNs (Merity et al., 2018)	–	–	33.0
Adaptive Transformer (Sukhbaatar et al., 2019)	36	8	20.6
Local Transformer	16	16	19.8
Adaptive Input (Baevski and Auli, 2019)	16	16	18.7
TransformerXL (Dai et al., 2019)	18	16	18.3
Routing Transformer	10	16	**15.8**

Table 2: Results on language modeling on `Wikitext-103` data-set. Local Transformer refers to Transformer (Vaswani et al., 2017) with relative position encoding (Shaw et al., 2018) together with local attention. Perplexity is reported on the test set.

Model	Layers	Heads	Bits per byte
T64 (Al-Rfou et al., 2019)	64	2	1.13
Local Transformer	24	8	1.10
TransformerXL (Dai et al., 2019)	24	8	0.99
Sparse Transformer (Child et al., 2019)	30	8	0.99
Adaptive Transformer (Sukhbaatar et al., 2019)	24	8	**0.98**
Routing Transformer	12	8	0.99

Table 3: Results on language modeling on `enwik-8` data-set. Local Transformer refers to Transformer (Vaswani et al., 2017) with relative position encoding (Shaw et al., 2018) together with local attention. Bits per byte (bpc) is reported on the test set.

Model	Layers	Heads	Bits/dim
Glow (Kingma and Dhariwal, 2018)	–	–	3.81
PixelCNN (Van den Oord et al., 2016)	–	–	3.57
PixelSNAIL (Chen et al., 2018)	–	–	3.52
SPN (Menick and Kalchbrenner, 2018)	–	–	3.52
ImageTransformer (Parmar et al., 2018)	24	16	3.48
Sparse Transformer (Child et al., 2019)	48	16	3.44
Reformer (Kitaev et al., 2020)	–	–	3.65
Routing Transformer	24	16	**3.43**

Table 4: Results on image generation on `ImageNet- 64` in bits/dim.

linear warmup over 10,000 steps followed by a *rsqrt_normalized_decay*. We do not make use of any dropout, or weight decay. The hidden dimension of our model is 1032 and the batch size is 8192 tokens.

From Table 5, we see that Local Transformer again sets a very strong baseline, with a 24-layer local attention model obtaining a test set perplexity of 39.3, while a 36-layer Transformer-XL gets 36.3. Moreover, a 22-layer Routing Transformer model improves on the 36-layer Compressive Transformer, obtaining a test set perplexity of 33.2 compared to 33.6, while being able to generate sequences of length 8192.

6 Analysis

6.1 Local vs Global

As reported in Section 5, a scaled up version of local attention is a strong baseline for efficient attention over long sequences. From Table 1 we see that local attention is slightly worse than full attention - 3.009 vs 2.983 bits per dim. Adding 2

Model	Layers	Heads	Perplexity
Local Transformer	24	8	39.3
TransformerXL (Dai et al., 2019)	36	–	36.3
Compressive Transformer (Rae et al., 2020)	36	–	33.6
Routing Transformer	22	8	**33.2**

Table 5: Results on language modeling on `PG-19` data-set. Local Transformer refers to Transformer (Vaswani et al., 2017) with relative position encoding (Shaw et al., 2018) together with local attention. Perplexity is normalized by the number of tokens reported in (Rae et al., 2020) and is reported on the test set.

	$\text{JSD}(local \| local)$	$\text{JSD}(local \| routing)$	$\text{JSD}(routing \| routing)$
`layer 0`	0.0038 ± 0.0018	0.4706 ± 0.0319	0.1579 ± 0.0576
`layer 1`	0.3071 ± 0.1217	0.6674 ± 0.0153	0.5820 ± 0.0104
`layer 2`	0.2164 ± 0.0803	0.5896 ± 0.0249	0.4015 ± 0.0121
`layer 3`	0.1163 ± 0.0336	0.6047 ± 0.0181	0.4144 ± 0.0264
`layer 4`	0.1840 ± 0.0562	0.6266 ± 0.0062	0.4191 ± 0.0879
`layer 5`	0.2284 ± 0.0225	0.6463 ± 0.0155	0.4687 ± 0.0449
`layer 6`	0.1901 ± 0.0525	0.6471 ± 0.0040	0.5175 ± 0.0469
`layer 7`	0.1566 ± 0.0685	0.5798 ± 0.0235	0.4350 ± 0.0139
`layer 8`	0.1638 ± 0.0739	0.5993 ± 0.0148	0.4268 ± 0.0291
`layer 9`	0.2095 ± 0.0560	0.6127 ± 0.0053	0.3581 ± 0.0019

Table 6: Jensen-Shannon divergence between the attention distributions of a random local attention head and a random head that routes attention as in Section 4.1 per layer on the `Wikitext-103` data-set. We report means and standard deviations computed over 10 runs and use the natural logarithm so that divergences are upper-bounded by 0.6931.

routing layers with 4 heads almost closes the gap with the performance of full attention, achieving 2.986 bits per dim. Adding more routing layers and heads improves performance up to a point, with the best performing model with an attention window of 512 having 4 routing layers and 4 routing heads, and achieving 2.975 bits per dim. Increasing the attention window from 512 to 1024 uniformly results in improvement in every setting. The best model on `CIFAR-10` has an attention window of 1024 with 4 routing layers and 4 routing heads. Interestingly, the best Routing Transformer models perform better than full attention, but not by a large enough amount to rule out noise. More importantly, Table 1 shows the importance of local attention in building intermediate representations, with a model with only routing attention layers and heads with attention windows of 512 and 1024 achieving 3.400 and 3.291 bits per dim respectively.

Thus Table 1 shows us the importance of local representations, as well as the benefit of adding a few routing layers and heads to enforce a more global representation. Because attention weights are a probability distribution on the entire set of tokens, we evaluate the difference in attention patterns between local and routing attention by computing the Jensen-Shannon divergence between the two kinds of attention distributions for a random subset of heads in our network on the `Wikitext-103` data-set. The divergence is computed over the entire sequence length of 4096. We average over 10 runs and report means and standard deviations of the JSD in Table 6. Note that the JSD is always non-negative and is upper-bounded by 0.6931 when computed using the natural logarithm. We observe that the divergence between the different local heads is always very low compared to the divergence between local and routing attention heads, which is almost always very close to the upper-bound of 0.6931. Divergence between different routing attention heads falls somewhere in between, being closer to the upper-bound. This shows that the attention distribution inferred by the routing attention of Section 4.1 is highly non-local in nature and different heads specialize in attending to very different parts of the input.

Model	Dataset	Seq. length	Layers	Heads	Attention window	Steps/sec
Local Transformer	PG-19	8192	24	8	512	1.231
Routing Transformer	PG-19	8192	22	8	512	0.7236

Table 7: Step time comparison between Local Transformer and Routing Transformer on a TPUv3 for the PG-19 data-set.

Qualitatively, from the ablations in Table 1, we hypothesize that the reason for the strong performance of the Routing Transformer is due to the fact that it combines building local representations over several layers, together with enforcing global consistency for every token. This is achieved via an approximate MIPS over the entire set of tokens (see Section 4.1), and selecting pairs that have a high dot product for attention. This allows various entities such as gender, nouns, dates and names of places to be consistent throughout the entire sequence, since on expectation the dot product similarity between similar entities are high, while for differing entities they are expected to be low. Essentially, we conjecture that for every time step, the prediction depends on a small support of *high value* tokens: Local attention facilitates local consistency and fluency, while a full dot product attention would facilitate global consistency. However, for long sequences, since full attention is infeasible, we believe that using spherical k-means to perform a MIPS search over the global set of tokens and performing attention between these high dot product items is a good approximation to *full dot product attention*. The importance of the MIPS search to select high dot product items is highlighted from the ablation in Table 1, where we see that a Random Transformer performs worse compared to a Local Transformer and a Routing Transformer with the same configuration (3.076 vs 3.009 vs 2.971 bits/dim).

6.2 Recurrence vs Sparse Attention

We also note that sparse attention is an orthogonal approach to that of Transformer-XL and Compressive Transformer, which train on small sequences and by performing careful cross attention over cached previous chunks hope to generalize to longer sequences. By contrast, we directly train on long sequences from the beginning—for example, the Compressive Transformer trains on chunks of size 512 for PG-19, while we train on sequences of length 8192. The benefit of the Transformer-XL like approach is that it is less memory consuming and thus is able to scale to 36 layers. Sparse attention (including local attention) on the other hand is more memory expensive since it trains directly on long sequences and therefore can scale to fewer layers for the same problem. However, as we demonstrate, it is competitive with the Transformer-XL like approaches even when using fewer layers and is guaranteed to generalize to the long sequence length that it was trained on.

6.3 Wall-Clock Time

We compare the step times for training the various sparse attention models on the CIFAR-10 data-set in Table 1 as well as on the PG-19 data-set in Table 7. For PG-19 we report only a comparison between the Local Transformer and the Routing Transformer, since sequence lengths are 8192 and performing full attention is infeasible. All the step time comparisons are made on a TPUv3, with the same number of cores and batch sizes to facilitate a fair comparison. As we see from Table 1, local attention is much faster than full attention, training at 9.023 steps per second compared to 5.608 steps per second. The Routing Transformer models on CIFAR-10 have step times that depend on the number of routing heads, with the best performing model with the same attention budget as local attention (i.e., an attention window of 512), which has 8 routing layers and 4 routing heads, training at 5.140 steps per second. Other Routing Transformer models are faster while still matching full attention, for example, 2 routing layers with 4 routing heads trains at 7.409 steps per second. Therefore, Local Transformer is roughly between $1.22 - 1.76\times$ faster than the best performing Routing Transformers. On the other hand Transformer is between $0.76 - 1.09\times$ faster than the best Routing Transformers.

On PG-19, we see from Table 7 that the Local Transformer is roughly $1.7\times$ faster compared to the Routing Transformer, similar to the trend on CIFAR-10. This trade-off with respect to speed

compared to the Local Transformer is due to the lack of support for sparse operations on the TPU; on the GPU various sparse kernels have been proposed which promise to significantly speed up training of these models (Gale et al., 2020). Note that our goal in this work is a memory efficient version of sparse attention that can well approximate full attention for long sequences; wall-clock time efficiency is only a secondary goal.

7 Conclusion

Transformer models constitute the state-of-the-art in auto-regressive generative models for sequential data. Their space-time complexity is, however, quadratic in sequence length, due to their attention modules. Our work proposes a sparse attention model, the Routing Transformer. It relies on content-based sparse attention motivated by non-negative matrix factorization. Compared with local attention models, it does not require fixed attention patterns but enjoys similar space-time complexity. In contrast with prior work on content-based sparse attention, it does not require computing a full attention matrix but still selects sparsity patterns based on content similarity.

Our experiments over text and image generation draw two main conclusions. First, we show that a scaled up version of local attention establishes a strong baseline on modern benchmark, even compared to recent state-of-the-art models. Second, we show that the Routing Transformer redefines the state-of-the-art in large long sequence benchmarks of `Wikitext-103`, `PG-19` and `ImageNet-64`, while being very close to do so on `enwik-8` as well. Our analysis also shows that routing attention modules offer complementary attention patterns when compared to local attention.

Overall, our work contributes an efficient attention mechanism that applies to the modeling of long sequences and redefines the state of the art for auto-regressive generative modeling. Our approach could prove useful in domains where the inputs are naturally sparse, such as 3D point clouds, social networks, or protein interactions.

Acknowledgments

The authors would like to thank Phillip Wang and Aran Komatsuzaki for a Pytorch implementation of Routing Transformer. The authors would also like to thank Yonghui Wu, Weikang Zhou, and Dehao Chen for helpful feedback in improving the implementation of this work. The authors would also like to thank anonymous reviewers and the Action Editor of TACL for their constructive comments, which helped improve the exposition of this work.

References

Rami Al-Rfou, Dokook Choe, Noah Constant, Mandy Guo, and Llion Jones. 2019. Character-level language modeling with deeper self-attention. In *Proceedings of the AAAI Conference on Artificial Intelligence*, volume 33, pages 3159–3166. **DOI:** `https://doi.org/10.1609/aaai.v33i01.33013159`

Alex Auvolat, Sarath Chandar, Pascal Vincent, Hugo Larochelle, and Yoshua Bengio. 2015. Clustering is efficient for approximate maximum inner product search. *arXiv preprint arXiv:1507.05910*.

Jimmy Lei Ba, Jamie Ryan Kiros, and Geoffrey E. Hinton. 2016. Layer normalization. *arXiv preprint arXiv:1607.06450*.

Alexei Baevski and Michael Auli. 2019. Adaptive input representations for neural language modeling. In *International Conference on Learning Representations*.

Dzmitry Bahdanau, Kyunghyun Cho, and Yoshua Bengio. 2015. Neural machine translation by jointly learning to align and translate. In *3rd International Conference on Learning Representations, ICLR 2015*.

Arindam Banerjee and Joydeep Ghosh. 2004. Frequency-sensitive competitive learning for scalable balanced clustering on high-dimensional hyperspheres. *IEEE Transactions on Neural Networks*, 15(3):702–719. **DOI:** `https://doi.org/10.1109/TNN.2004.824416`, **PMID:** 15384557

Yoshua Bengio, Nicholas Léonard, and Aaron Courville. 2013. Estimating or propagating gradients through stochastic neurons for conditional computation. *arXiv preprint arXiv:1308.3432*.

Mathieu Blondel, André F. T. Martins, and Vlad Niculae. 2019. Learning classifiers with

fenchel-young losses: Generalized entropies, margins, and algorithms. In *The 22nd International Conference on Artificial Intelligence and Statistics, AISTATS 2019, 16–18 April 2019, Naha, Okinawa, Japan*, pages 606–615.

Leon Bottou and Yoshua Bengio. 1995. Convergence properties of the k-means algorithms. In *Advances in Neural Information Processing Systems*, pages 585–592.

Xi Chen, Nikhil Mishra, Mostafa Rohaninejad, and Pieter Abbeel. 2018. Pixelsnail: An improved autoregressive generative model. In *International Conference on Machine Learning*, pages 864–872.

Rewon Child, Scott Gray, Alec Radford, and Ilya Sutskever. 2019. Generating long sequences with sparse transformers. *arXiv preprint arXiv:1904.10509*.

Chung-Cheng Chiu and Colin Raffel. 2018. Monotonic chunkwise attention. In *6th International Conference on Learning Representations, ICLR 2018, Vancouver, BC, Canada, April 30 - May 3, 2018, Conference Track Proceedings*. OpenReview.net.

Kyunghyun Cho and Yoshua Bengio. 2014. Exponentially increasing the capacity-to-computation ratio for conditional computation in deep learning. *arXiv preprint arXiv:1406.7362*.

Kyunghyun Cho, Bart van Merriënboer, Caglar Gulcehre, Dzmitry Bahdanau, Fethi Bougares, Holger Schwenk, and Yoshua Bengio. 2014. Learning phrase representations using rnn encoder–decoder for statistical machine translation. In *Proceedings of the 2014 Conference on Empirical Methods in Natural Language Processing (EMNLP)*, pages 1724–1734.

Jan K. Chorowski, Dzmitry Bahdanau, Dmitriy Serdyuk, Kyunghyun Cho, and Yoshua Bengio. 2015. Attention-based models for speech recognition. In *Advances in Neural Information Processing Systems*, pages 577–585.

Gonçalo M. Correia, Vlad Niculae, and André F. T. Martins. 2019. Adaptively sparse transformers. In *Proceedings of the 2019 Conference on Empirical Methods in Natural Language Processing and the 9th International Joint Conference on Natural Language Processing (EMNLP-IJCNLP)*, pages 2174–2184. **DOI:** `https://doi.org/10.18653/v1/D19-1223`

Zihang Dai, Zhilin Yang, Yiming Yang, Jaime G. Carbonell, Quoc Le, and Ruslan Salakhutdinov. 2019. Transformer-xl: Attentive language models beyond a fixed-length context. In *Proceedings of the 57th Annual Meeting of the Association for Computational Linguistics*, pages 2978–2988.

Ludovic Denoyer and Patrick Gallinari. 2014. Deep sequential neural network. *arXiv preprint arXiv:1410.0510*.

Jacob Devlin, Ming-Wei Chang, Kenton Lee, and Kristina Toutanova. 2019. BERT: Pre-training of deep bidirectional transformers for language understanding. In *NAACL-HLT (1)*.

David Eigen, Marc'Aurelio Ranzato, and Ilya Sutskever. 2013. Learning factored representations in a deep mixture of experts. *arXiv preprint arXiv:1312.4314*.

Trevor Gale, Matei Zaharia, Cliff Young, and Erich Elsen. 2020. Sparse GPU kernels for deep learning. *arXiv preprint arXiv:2006.10901*.

Edouard Grave, Armand Joulin, and Nicolas Usunier. 2017. Improving neural language models with a continuous cache. In *5th International Conference on Learning Representations, ICLR 2017, Toulon, France, April 24-26, 2017, Conference Track Proceedings*. OpenReview.net.

Alex Graves, Greg Wayne, and Ivo Danihelka. 2014. Neural turing machines. *arXiv preprint arXiv:1410.5401*.

Karol Gregor, Ivo Danihelka, Alex Graves, Danilo Jimenez Rezende, and Daan Wierstra. 2015. DRAW: A recurrent neural network for image generation. Francis R. Bach and David M. Blei, editors, In *Proceedings of the 32nd International Conference on Machine Learning, ICML 2015, Lille, France, 6-11 July 2015*, volume 37 of *JMLR Workshop and Conference Proceedings*, pages 1462–1471. JMLR.org.

Ari Holtzman, Jan Buys, Li Du, Maxwell Forbes, and Yejin Choi. 2020. The curious case of neural text degeneration. In *International Conference on Learning Representations*.

Cheng-Zhi Anna Huang, Ashish Vaswani, Jakob Uszkoreit, Ian Simon, Curtis Hawthorne, Noam Shazeer, Andrew M. Dai, Matthew D. Hoffman, Monica Dinculescu, and Douglas Eck. 2018. Music transformer: Generating music with long-term structure. In *International Conference on Learning Representations*.

Sathish Reddy Indurthi, Insoo Chung, and Sangha Kim. 2019. Look harder: A neural machine translation model with hard attention. In *Proceedings of the 57th Conference of the Association for Computational Linguistics*, pages 3037–3043. **DOI:** https://doi.org/10.18653/v1/P19-1290

Navdeep Jaitly, Quoc V. Le, Oriol Vinyals, Ilya Sutskever, David Sussillo, and Samy Bengio. 2016. An online sequence-to-sequence model using partial conditioning. In *Advances in Neural Information Processing Systems*, pages 5067–5075.

Diederik P. Kingma and Jimmy Ba. 2015. Adam: A method for stochastic optimization. Yoshua Bengio and Yann LeCun, editors, In *3rd International Conference on Learning Representations, ICLR 2015, San Diego, CA, USA, May 7-9, 2015, Conference Track Proceedings*.

Durk P. Kingma and Prafulla Dhariwal. 2018. Glow: Generative flow with invertible 1x1 convolutions. In *Advances in Neural Information Processing Systems*, pages 10215–10224.

Nikita Kitaev, Lukasz Kaiser, and Anselm Levskaya. 2020. Reformer: The efficient transformer. In *International Conference on Learning Representations*.

Guillaume Lample, Alexandre Sablayrolles, Marc'Aurelio Ranzato, Ludovic Denoyer, and Hervé Jégou. 2019. Large memory layers with product keys. In *Advances in Neural Information Processing Systems*, pages 8548–8559.

Peter J. Liu, Mohammad Saleh, Etienne Pot, Ben Goodrich, Ryan Sepassi, Lukasz Kaiser, and Noam Shazeer. 2018. Generating wikipedia by summarizing long sequences. In *International Conference on Learning Representations*.

Xiaodong Liu, Pengcheng He, Weizhu Chen, and Jianfeng Gao. 2019. Multi-task deep neural networks for natural language understanding. In *Proceedings of the 57th Annual Meeting of the Association for Computational Linguistics*, pages 4487–4496.

Minh-Thang Luong, Hieu Pham, and Christopher D. Manning. 2015. Effective approaches to attention-based neural machine translation. In *Proceedings of the 2015 Conference on Empirical Methods in Natural Language Processing*, pages 1412–1421. **DOI:** https://doi.org/10.18653/v1/D15-1166

Matt Mahoney. 2011. Large text compression benchmark. *URL:* http://www.mattmahoney.net/text/text.html

Chaitanya Malaviya, Pedro Ferreira, and André F. T. Martins. 2018. Sparse and constrained attention for neural machine translation. In *Proceedings of the 56th Annual Meeting of the Association for Computational Linguistics (Volume 2: Short Papers)*, pages 370–376, Melbourne, Australia. Association for Computational Linguistics. **DOI:** https://doi.org/10.18653/v1/P18-2059

Mikko I. Malinen and Pasi Fränti. 2014. Balanced k-means for clustering. In *Joint IAPR International Workshops on Statistical Techniques in Pattern Recognition (SPR) and Structural and Syntactic Pattern Recognition (SSPR)*, pages 32–41. Springer. **DOI:** https://doi.org/10.1007/978-3-662-44415-3_4

André F. T. Martins and Julia Kreutzer. 2017. Learning what's easy: Fully differentiable neural easy-first taggers. In *Proceedings of the 2017 Conference on Empirical Methods in Natural Language Processing*, pages 349–362, Copenhagen, Denmark. Association for Computational Linguistics. **DOI:** https://doi.org/10.18653/v1/D17-1036

Jacob Menick and Nal Kalchbrenner. 2018. Generating high fidelity images with subscale pixel networks and multidimensional upscaling. In *International Conference on Learning Representations*.

Stephen Merity, Nitish Shirish Keskar, and Richard Socher. 2018. An analysis of neural language modeling at multiple scales. *arXiv preprint arXiv:1803.08240*.

Stephen Merity, Caiming Xiong, James Bradbury, and Richard Socher. 2017. Pointer sentinel mixture models. In *5th International Conference on Learning Representations, ICLR 2017, Toulon, France, April 24-26, 2017, Conference Track Proceedings*. OpenReview.net.

Niki Parmar, Ashish Vaswani, Jakob Uszkoreit, Lukasz Kaiser, Noam Shazeer, Alexander Ku, and Dustin Tran. 2018. Image transformer. In *International Conference on Machine Learning*, pages 4055–4064.

Alec Radford, Karthik Narasimhan, Tim Salimans, and Ilya Sutskever. 2018. Improving language understanding by generative pre-training. *URL* https://s3-us-west-2.amazonaws.com/openai-assets/research-covers/languageunsupervised/languageunderstandingpaper.pdf

Jack Rae, Jonathan J. Hunt, Ivo Danihelka, Timothy Harley, Andrew W. Senior, Gregory Wayne, Alex Graves, and Timothy Lillicrap. 2016. Scaling memory-augmented neural networks with sparse reads and writes. In *Advances in Neural Information Processing Systems*, pages 3621–3629.

Jack Rae and Ali Razavi. 2020. Do transformers need deep long-range memory? In *Proceedings of the 58th Annual Meeting of the Association for Computational Linguistics*, pages 7524–7529. Association for Computational Linguistics. Online. **DOI:** https://doi.org/10.18653/v1/2020.acl-main.672

Jack W. Rae, Anna Potapenko, Siddhant M. Jayakumar, Chloe Hillier, and Timothy P. Lillicrap. 2020. Compressive transformers for long-range sequence modelling. In *International Conference on Learning Representations*.

Peter Shaw, Jakob Uszkoreit, and Ashish Vaswani. 2018. Self-attention with relative position representations. In *Proceedings of the 2018 Conference of the North American Chapter of the Association for Computational Linguistics: Human Language Technologies, Volume 2 (Short Papers)*, pages 464–468. **DOI:** https://doi.org/10.18653/v1/N18-2074

Noam Shazeer, Azalia Mirhoseini, Krzysztof Maziarz, Andy Davis, Quoc V. Le, Geoffrey E. Hinton, and Jeff Dean. 2017. Outrageously large neural networks: The sparsely-gated mixture-of-experts layer. In *5th International Conference on Learning Representations, ICLR 2017, Toulon, France, April 24-26, 2017, Conference Track Proceedings*. OpenReview.net.

Noam Shazeer and Mitchell Stern. 2018. Adafactor: Adaptive learning rates with sublinear memory cost. In *International Conference on Machine Learning*, pages 4596–4604.

Sainbayar Sukhbaatar, Édouard Grave, Piotr Bojanowski, and Armand Joulin. 2019. Adaptive attention span in transformers. In *Proceedings of the 57th Annual Meeting of the Association for Computational Linguistics*, pages 331–335. **DOI:** https://doi.org/10.18653/v1/P19-1032

Aaron Van den Oord, Nal Kalchbrenner, Lasse Espeholt, Oriol Vinyals, Alex Graves, and others. 2016. Conditional image generation with PixelCNN decoders. In *Advances in Neural Information Processing Systems*, pages 4790–4798.

Ashish Vaswani, Noam Shazeer, Niki Parmar, Jakob Uszkoreit, Llion Jones, Aidan N. Gomez, Łukasz Kaiser, and Illia Polosukhin. 2017. Attention is all you need. In *Advances in Neural Information Processing Systems*, pages 5998–6008.

Kelvin Xu, Jimmy Ba, Ryan Kiros, Kyunghyun Cho, Aaron C. Courville, Ruslan Salakhutdinov, Richard S. Zemel, and Yoshua Bengio. 2015. Show, attend and tell: Neural image caption generation with visual attention. Francis R. Bach and David M. Blei, editors, In *Proceedings of the 32nd International Conference on Machine Learning, ICML 2015, Lille, France, 6-11 July 2015*, volume 37 of *JMLR Workshop and Conference Proceedings*, pages 2048–2057. JMLR.org.

Zhilin Yang, Zihang Dai, Yiming Yang, Jaime Carbonell, Russ R Salakhutdinov, and Quoc V. Le. 2019. XLNet: Generalized autoregressive pretraining for language understanding. In *Advances in Neural Information Processing Systems*, pages 5753–5763.